Asian Journal of Chemistry; Vol. 27, No. 11 (2015), 4291-4296

ASIAN JOURNAL OF CHEMISTRY

http://dx.doi.org/10.14233/ajchem.2015.19514

Numerical Analysis of Droplet Formation and Effect of Ink Properties in Shear-Type Piezoelectric Inkjet Printhead†

KYOUNGWOO PARK[1,*], CHOL-HO HONG[1], BYEONG-SAM KIM[1] and HEONCHANG KIM[2]

[1]School of Mechanical Engineering, Hoseo University, Asan-si, Chungnam 336-795, Republic of Korea
[2]Department of Chemical Engineering, Hoseo University Asan-si, Chungnam 336-795, Republic of Korea

*Corresponding author: Fax:+ 82 41 5405808; Tel: +82 41 5405804; E-mail: kpark@hoseo.edu

AJC-17461

In digital textile printing (DTP) system, the selection of inkjet printhead is one of the core technologies. The printing quality such as the volume and velocity of droplets as well as the formation of satellite droplets is known to be closely related to the injection behaviours of the ink droplet. In the present work, we investigate the droplet behaviour of micro-inkjet for shear-mode piezoelectric (PZT) actuators numerically. The transient three-dimensional conservation equations of mass and momentum are solved by the computational fluid dynamics. The continuous surface force model is used in order to predict the effect of surface tension force in the free surface flow. The volume-of-fluid method with the piecewise linear interface construction scheme is employed both for tracking the interfacial movement and reconstructing the interface between liquid and gas (*i.e.*, ink and air). This study predict the droplet formation characteristics for the given properties of ink and geometry of printhead and the effects of thermal properties of ink and nozzle shape on the droplet quality are also investigated.

Keywords: Computational fluid dynamics, Shear-mode piezoelctric actuator, Interfacial phenomena, Droplet behaviour.

INTRODUCTION

The inkjet printing technology, which was originally developed to apply conventional computer printers, has received considerable attention in many other industrial applications such as a non-contact deposition of liquid crystal display (LCD), organic light-emitting diode (OLED) and a photoresist coating technique by droplet generator due to its high-resolution, multi-color patterning and lateral patterning capability.

According to the actuating mechanism, the inkjet printing technology can be divided into electrostatic, thermal, acoustic and piezoelectric inkjet (PIJ) printheads[1]. Among them piezoelectric inkjet technology has many advantages such as easy control of the droplet volume, more flexible in the ink compatibility and higher range in the operation frequency. Depending on the actuator configuration, directions of lead zirconate titanate (PZT) polarization and electric field between the electrodes, the piezoelectric inkjet can be further classified into four types: squeeze, push, shear and bend modes[2]. Irrespective of inkjet technologies, the printing quality is known to be closely related to that of the ejected droplet so that it is desirable to reduce droplet size, to improve droplet repeatability and to increase operation frequency and droplet velocity.

For the design of the droplet formation and its ejection process in piezoelectric inkjet printing, numerical simulations have been employed by a number of researchers[3-5]. Fromm[3] studied on the evolution of ejected droplets with the actuation through a driving pressure numerically. In this study he used the vorticity-stream function form of the Navier-Stokes equation to solve the droplet mechanism. Pan *et al.*[4] discussed the numerical simulation on the drop formation process for the design of a MEMS diaphragm drop ejector. They addressed the fluid-structure interaction between the pressure of the fluid and the motion of the actuator diaphragm and solved it in a 2D axisymmetric domain through Flow3D. The 3D simulation of the liquid ejection behaviour for a Picojet printhead was reported by Yang *et al.*[5]. They used the continuous surface force (CSF) scheme in order to treat the surface tension effect at the gas-liquid boundary and employed the volume-of-fluid (VOF) method to describe the behaviour of the interfacial movements.

†Presented at The 8th ICMMA-2014, held on 27-29 November 2014, Hoseo University, Chungnam, Republic of Korea

In the present work, the mechanisms of droplet formation and its ejection of the PZT actuated droplet generator are investigated numerically. To predict the droplet ejection phenomenon in simulating interfacial flow fields involving inertia, capillarity, free-surface movement and unsteady state, a commercial computational fluid dynamics software of STAR-CCM+ was utilized in numerical calculation. The formation and ejection of main droplet included the satellite droplet are studied and the effects of the design parameters (*i.e.*, nozzle diameter, nozzle plate thickness), ink properties (*i.e.*, viscosity, surface tension coefficient) and the driving condition of pressure distribution at inlet on the inkjet performance such as the droplet size and velocity are also investigated numerically.

MATHEMATICAL MODEL

Physical configuration: The PZT-driven inkjet printhead considered in the study is schematically shown in Fig. 1. As shown this figure, the printhead consists of a PZT transducer, a diaphragm, a pressure chamber (or ink flow chamber) and a nozzle plate. The contraction or expansion of the PZT (piezoelectric actuator), which is occurred by the applied voltage pulse, causes an instantaneous change in the pressure distribution within the printhead. The change of pressure is converted into velocity variation according to the time and this acts as the driving force. Table-1 shows the dimensions used in this study. In the table, H_4 means the free surface height surrounded by air, that is, the distance from nozzle exit to the target.

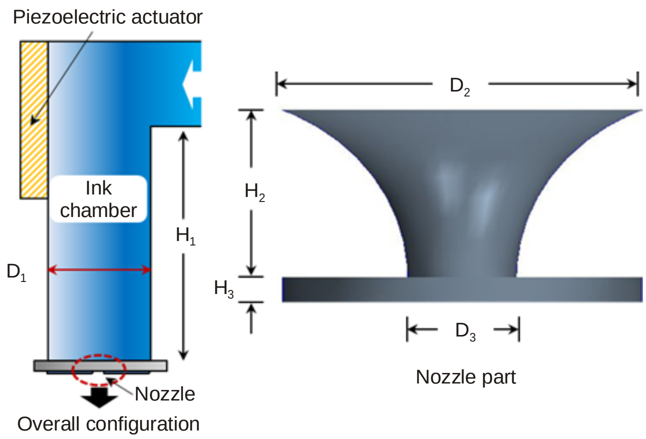

Fig. 1. A schematic diagram of a shear-mode piezoelectric inkjet printhead

TABLE-1
DIMENSIONS OF PIEZOELECTRIC INKJET PRINTHEAD CONSIDERED IN THE STUDY

Dimensions	Values (μm)	Fluid
Chamber height, H_1	4,700	Liquid
Chamber diameter, D_1	205	
Nozzle height, H_2	64	Liquid
Nozzle plate thickness, H_3	5	
Nozzle diameter (upper), D_2	122	
Nozzle diameter (lower), D_3	37	
Free surface height, H_4	1,000	Liquid-Gas
Free surface diameter, D_4	662	

Governing equations: For the prediction of droplet formation and ejection mechanism in the shear-mode piezoelectric inkjet printhead, the transient three-dimensional conservation equations of mass and momentum are solved, simultaneously.

The ink solution is assumed to be incompressible, homogeneous, isothermal with gravity effects and constant surface tension coefficient (σ) and contact angle. As we expected, the inkjet ejection phenomenon is a complicated flow of two immiscible fluids liquid and gas (*i.e.*, ink and air) so that the surface tension of the ink plats an important role on the droplet behaviour. The continuity and Navier-Stokes equations governing the droplet evolution can be expressed in the following tensor forms,

$$\frac{\partial \rho}{\partial t}+\frac{\partial}{\partial x_j}(\rho u_i)=0 \quad (1)$$

$$\frac{\partial}{\partial t}(\rho u_i)+\frac{\partial}{\partial x_j}(\rho u_i u_j)=-\frac{\partial p}{\partial x_i}+\frac{\partial}{\partial x_j}\left[\mu\left(\frac{\partial u_i}{\partial x_j}+\frac{\partial u_j}{\partial x_i}\right)\right]+\rho g_i+F_i^{\sigma} \quad (2)$$

where ρ is the fluid density specified as 1,170 and 1.184 kg/m^3 for liquid and gas, respectively, t the time, u_i the velocity in the direction of x_i, p the pressure and μ the viscosity as 8.6 × 10^{-3} and 1.85 × 10^{-5} N·s/m^2 for liquid and air, respectively. The terms ρg_i and F_i^{σ} in eqn. 2 denote the gravitational force and the volumetric force of liquid surface tension in the direction of x_i, respectively.

To describe the behaviour interfacial movements, the volume-of-fluid (VOF) method[6] with the piecewise linear interface construction (PLIC) technique[7] is used in this work. From the law of mass conservation, the liquid volume fraction, f, according to the volume-of-fluid method, is governed by the following equation:

$$\frac{\partial f}{\partial t}+\frac{\partial}{\partial x_j}(f u_i)=0 \quad (3)$$

Note that f = 1 and f = 0 for the grid cells are filled by liquid and gas, respectively and for 0 < f < 1, the grid cell contains both liquid and gas. To calculate the physical properties such as density (ρ) and viscosity (μ) in each computational cell, the average values of mixture can be determined using the following mixing rule with the known f,

$$\rho = f\rho_l+(1-f)\rho_g, \quad \mu=\frac{f\rho_l\mu_l+(1-f)\rho_g\mu_g}{\rho} \quad (4)$$

The subscripts *l* and g mean the liquid and gas phases, respectively.

The surface tension effect at the air-ink boundary as shown in eqn. 2 is treated by the continuous surface force (CSF) scheme to track the interface location[8]. This model uses the gradient of f to define the normal vector at the interface pointing from gas to liquid. The surface tension, F_i^{σ}, is calculated by the following equation:

$$F_i^{\sigma}=-\sigma\left[\frac{\partial}{\partial x_j}\left(\frac{\partial f}{\partial x_j}\Big/\left|\frac{\partial f}{\partial x_j}\right|\right)\right]\left(\frac{\partial f}{\partial x_i}\right) \quad (5)$$

Initial and boundary conditions: The expansion and contraction of the PZT causes the propagation of a pressure wave within the ink chamber and it convert into a velocity as the function of time. The ink is ejected by the generated velocity through the nozzle. In the present study, the following equation is used the boundary condition at the printhead inlet.

$$u_{inlet} = V_a e^{-\beta t} \sin(\omega t) \quad (6)$$

where V_a is the average velocity and it is obtained both by a real droplet behaviour and a dynamic characteristic at the piezoelectric actuator. β is the damping coefficient, t the time and ω the frequency. No-slip boundary condition is employed at the solid walls and the pressure boundary condition is used at the ambient area out of the nozzle. The surface tension of the liquid and gas interface is calculated as follows:

$$F_i^{\sigma} = -\sigma\left(\frac{\partial n_j}{\partial x_j}\right)\left(\frac{\partial f}{\partial x_i}\right), \quad n_j = n_j^w \cos\theta_n + t_j^w \sin\theta_n \quad (7)$$

where n_j^w and t_j^w are the unit vectors, normal and tangential to the wall, respectively and θ_n represents the contact angle, which is assumed to be constant in the study ($\theta_n = 9°$).

The formation and ejection of inkjet droplet are occurred according to the time. That is, the problem considered in the study is unsteady state one so that the determination of time step size (δt) is very important. To select the time step, the explicit treatments of the convection term in Navier-Stokes equation (δt_c) and the surface tension term (δt_s) are considered simultaneously and they are given by

$$\delta t_c \le \frac{\delta x_i}{2\max(|u_j|)}, \quad \delta t_s < \left(\frac{(\rho_l + \rho_g)\delta x_j}{4\pi\sigma}\right)^{1/2} \quad (8)$$

The time step should be chosen to be smaller than δt_c and δt_s and in the present work, the time step size is 0.01 µs.

Numerical analysis: Numerical calculations are conducted with the computational fluid dynamics software of STAR-CCM+[9] to predict the mechanism of droplet formation and its ejection processes in the piezoelectric inkjet printhead. The grid system considered in the study is illustrated in Fig. 2 and it is composed of four structured sections such as the ink chamber, the nozzle, the nozzle plate and the outside the nozzle. Because the computational domain has a micro scale, the grid system is constructed firstly for the expanded configuration by ten times and then it completed by using the scale mesh in STAR-CCM+ (*i.e.*, the total number of grids is about 600,000). Finer grids are placed in the nozzle part as well as the region of droplet ejection with a smallest spacing of ** µm.

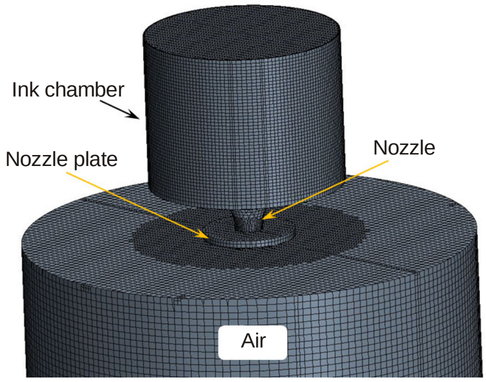

Fig. 2. Numerical grid system for the shear-mode piezoelectric inkjet printhead

The governing equations are discretized by the FVM and non-staggered variable arrangement is used. To compute the convection and diffusion terms, the power law scheme and the central difference scheme are used, respectively and the SIMPLE algorithm[10] is employed to resolve the pressure-velocity coupling problem. The final solutions are obtained when the residuals for all variables are less than 10^{-4}.

RESULTS AND DISCUSSION

Droplet ejection phenomenon: Fig. 3 illustrates the droplet ejection mechanism at every 10 µs. The working fluid is a commercial ink and its thermal properties of viscosity, density, surface tension coefficient for the base model are 1,170 kg/m³, 8.6×10^{-3} N·s/m² and 0.0353 N·m/m², respectively. The

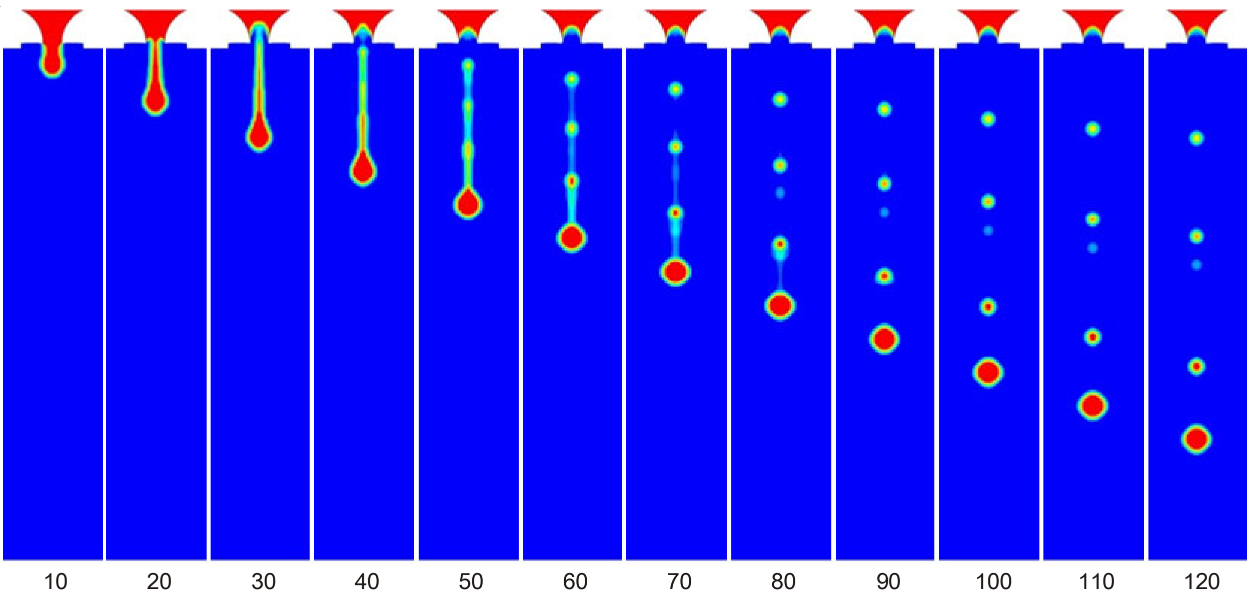

Fig. 3 Mechanism of the droplet formation and its ejection during 120

diameter of nozzle exit is 37 μ and the distance from nozzle exit to the target material is 1,000 μm. This figure clearly shows how the droplet is formed and how the droplet is ejected onto the substrate during 120 μs, that is, including expansion of the liquid protrusion, separation of the droplet from the nozzle (*i.e.* breakup of the droplet), creation of the satellite droplet and traveling the droplet to the target. As shown in Fig. 3, at around 25.7 μm, the liquid's forward inertia force overcomes the opposite effects of surface tension and viscous force so that one droplet breakup is completed with a tailing droplet (*i.e.*, called it as a satellite droplet). In this case, the breakup distance, which is defined as the distance from the nozzle exit to the fore-end of main droplet, is calculated as 117.06 μm. In addition, the droplet volume at t = 120 μs is estimated by 45.95 pl and it is calculated form the fact that a droplet is assumed to be a complete sphere shape with a measured radius in the result data of STAR-CCM+. The droplet velocity can be determined by using the different positions (l = 58.58 μm) at the time interval (t = 20 μs) along the droplet-moving direction and it turns out that the droplet velocity is 2.929 m/s for the base model. As we expected, the satellite droplet with a volume of 2.162 pl will become one with the main droplet on the substrate. In this situation, the distance between main and satellite droplets is obtained as 124.23 μm and it is one of the important factor for the printing quality because the satellite droplet may impact at a different position to the main droplet if the vibration in the print and the flow around the nozzle are occurred. Therefore, the shorter distance between main and satellite droplets can guarantee the better performance of the printing quality.

The formation of a liquid droplet and breakup phenomena of the droplet can be clearly observed by using the velocity

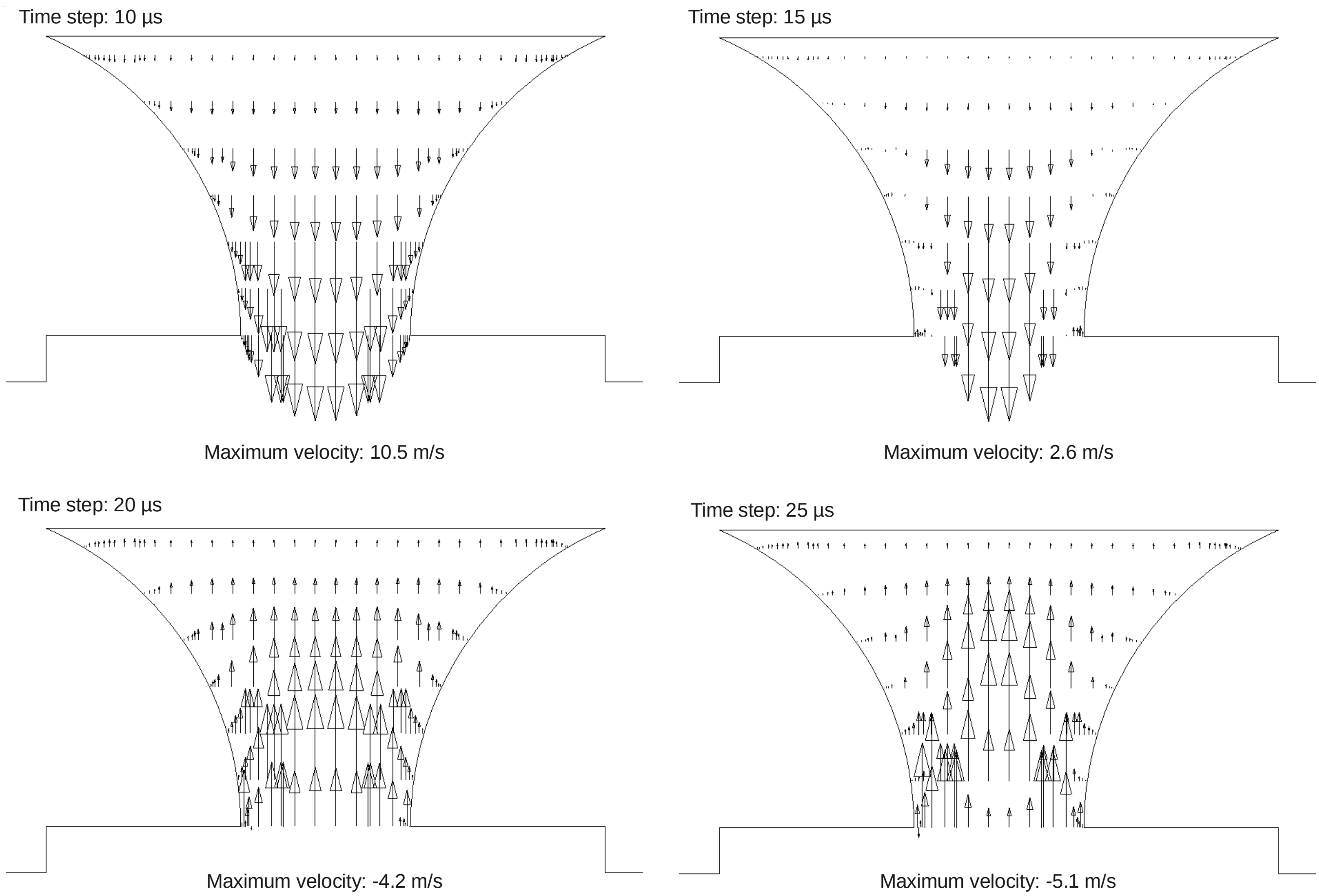

Fig. 4. Velocity vectors around the nozzle according to the time

TABLE-2
EFECT OF VISCOSITY ON THE PRINTHEAD PERFORMANCE

		Viscosity (μ), [unit: (10^{-3}) N·s/m]				
		6.5	7.5	8.6	9.5	10.5
Main droplet	Velocity, m/s	3.232	3.131	2.929	2.873	2.827
	Volume, pl	33.510	39.690	45.950	46.001	46.121
	Breakup time, μs	17.1	17.7	18.3	19.4	21.5
	Breakup distance, μm	120.40	118.71	117.06	106.36	105.43
Satellite droplet	Velocity, m/s	2.780	2.727	2.653	2.525	2.470
	Volume, pl	2.65	2.21	2.162	2.01	1.48
	Distance between main and satellite droplets at 100 μs	129.18	126.25	124.23	116.15	117.75

TABLE-4
EFFECT OF NOZZLE EXIT DIAMETER ON THE PRINTHEAD PERFORMANCE

		Nozzle exit diameter (d_3), [unit: µm]				
		25	30	37	45	50
Main droplet	Velocity, m/s	9.71	6.06	2.929	1.910	–
	Volume, pl	29.601	39.342	45.950	50.342	–
	Breakup time, µs	16.1	17.3	18.3	20.5	–
	Breakup distance, µm	181.8	135.34	117.06	82.82	–
Satellite droplet	Velocity, m/s	3.470	2.63	2.653	–	–
	Volume, pl	0.920	1.782	2.162	–	–
	Distance between main and satellite droplets at 100 µs	520.15	320.17	124.23	–	–

vector profile as the function of the time around the nozzle. The front views of the simulated velocity profiles according to the time around the nozzle are shown in Fig. 4 to illustrate the formation and breakup of the droplet. During 1-15 µs, the positive pressure on top of the ink chamber pushes the liquid in the nozzle and accelerates ($t < 5$ µs) and decelerates ($5 < t < 15$ µs) the liquid droplet. The negative pressure (or velocity) is generated around at $t > 20$ µs. This means that the necking-down of the ejected droplet occurs at the tip of the nozzle during $15 < t < 20$ µs due to the influences of both the upward pulling force and downward surface tension force. The breakup of the droplet from the nozzle is occurred (*i.e.*, the completed separation from the nozzle) during this time interval and the slender tail is formed due to the surface tension effect. In the present study, the breakup time is calculated as 18.3 µs for the base model.

Effect of ink properties: It is generally known that the droplet ejection is a complicated free surface flow of two immiscible fluids of liquid(ink) and gas(air). Table-2 illustrates the effect of ink viscosity ($\mu = 6.5 – 10.5 \times 10^{-3}$ [N·s/m]) on the printing quality such as velocity and volume of the droplet for the main and satellite droplets. As shown in Table-2, as viscosity of the ink increases, the velocity and volume of droplet decreases and increases, respectively. It is also found that high viscous liquid produces a relatively longer breakup time and slower droplet velocity because of the intensely viscous dissipation and the greater damping effect. This is also due to the fact that the increased viscous force dissipates the inertia force needed for ejecting ink out of nozzle. This means that the ink with a very high viscosity can fail to be ejected the droplet. Therefore, the selection of proper ink with viscosity becomes one of the important design parameters to improve the printing quality.

In the micro scale, the influence of gravity is less than that of surface tension during the droplet flying process. Therefore, the surface tension of the liquid plays a significant role on the droplet behaviour. The effect of surface tension coefficient (σ) on the velocity and volume of main droplet is illustrated in Fig. 5 at $d_3 = 37$ µm and $\mu = 8.6$ cP. It can be seen in the figure that the droplet velocity increases as the surface tension coefficient increases because the liquid with high surface tension can be cohered much more quickly into a spherical droplet shape due to the stronger capillary force. On the contrary, the volume of droplet becomes smaller as the influence of σ is stronger. Although it is not listed in this work, the breakup time and the breakup distance are decreased as the surface tension becomes larger because the downward pulling force becomes stronger. This opposite result suggests

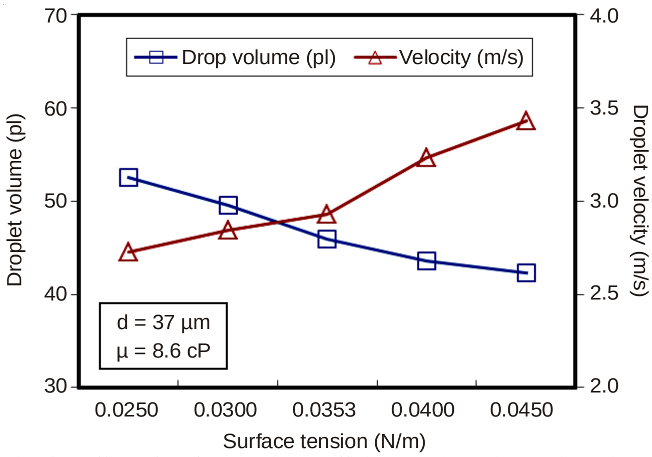

Fig. 5. Effect of surface tension coefficient on the main droplet volume and velocity

that it is needed to find the optimal ink with surface tension coefficient by using the optimization technology in the future.

Effect of nozzle shape: It is also known that the nozzle diameter has a strong influence on the droplet quality of piezoelectric inkjet printhead such as the droplet size and velocity. Table-3 lists the effect of the nozzle exit diameter (d_3 = 25-50 µm) on the droplet ejection behaviour for the base properties of the ink (*i.e.*, $\mu = 8.6$ cP and $\sigma = 0.0353$ N/m). As shown in the Table-3, a larger diameter of nozzle exit can cause a lower ejection velocity with a longer droplet breakup time. This indicates that the small size of nozzle diameter is better than that of larger one from the droplet velocity and volume point of view. This phenomenon results from the fact that the same amount of liquid mass, which is generated by the piezo diaphragm, is forced out from the nozzle. An interesting result is found that for the case of $d_3 = 50$ µm, both the main and satellite droplets cannot be generated due to the inadequate ejection velocity, which is explained by the mass conservation theory, within the parametric ranges of the present study. It can be also seen in Table-3 that the satellite droplet is not formed for the case of $d_3 = 45$ µm.

Conclusion

In the present study, the droplet formation and ejection processes for a shear-mode piezoelectric inkjet printhead have been investigated numerically. The numerical simulations were performed by the general purpose of computational fluid dynamics software of STAR-CCM+ with the CSF scheme for treating the surface tension effect at the gas-liquid boundary and the volume-of-fluid method with the piecewise linear interface construction technique for predicting the behaviour of interfacial movements. The printing quality is known to be closely related to those of the droplet size (volume, few Pico liters) and velocity as well as formation of satellite droplets. It is also known that the quality is strongly dependent on the nozzle shape and physical properties of ink. The major results are as follows; the droplet velocity increases with smaller nozzle diameter because of both a shorter droplet breakup time and a longer breakup length. For the case of over the diameter of d_3 = 45 μm, the droplet cannot be formed due to the insufficient ejection velocity. In addition, high viscosity causes the increase of breakup time to reduce the droplet velocity and it is also found that for the case of higher surface tension force the cohesive force is increased so that the shape of droplet is quickly formed as a spherical one and then the velocity of droplet is increased.

ACKNOWLEDGEMENTS

This work was supported by grant No.10047613 from the Components Technique Development with S/W Fusion Program (KEIT) of the Ministry of Trade, Industry and Energy (MOTIE).

REFERENCES

1. H.P. Le, *J. Imaging Sci. Technol.*, **42**, 49 (1998).
2. J. Brunahl and A.M. Grishin, *Sens. Actuators A*, **101**, 371 (2002).
3. J.E. Fromm, *IBM J. Res. Develop.*, **28**, 322 (1984).
4. F. Pan, J. Kubby and J. Chen, *J. Micromech. Microeng.*, **12**, 70 (2002).
5. A.S. Yang, J.C. Yang and M.C. Hong, *J. Micromech. Microeng.*, **16**, 180 (2006).
6. C.W. Hirt and B.D. Nichols, *J. Comput. Phys.*, **39**, 201 (1981).
7. D.L. Youngs, in eds.: K.W. Morton and M.I. Norman, Time-Dependent Multi-Material Flow with Large Fluid Distribution, In: Numerical Methods for Fluid Dynamics, pp. 187-221 (1986).
8. D.B. Kothe, W.J. Rider, S.J. Mosso, J.S. Brock and J.I. Hochstein, Volume Tracking of Interfaces having Surface Tension in Two and Three Dimensional, AIAA 96-0859.
9. STAR CCM+, User's guide, Release 8.02(2014), CD-Adapco.
10. S.V. Patankar, Numerical Heat Transfer and Fluid Flow, Hemisphere (1980).